

# Technical Report

## December 25, 2016, Mw=7.6, Chiloé Earthquake

Sergio Barrientos and the CSN team

On December 25, 2016 at 11:22 a.m. (local time) an Mw=7.6 earthquake took place on the coast of the Los Lagos Region, 67 km north-west of the town of Melinka, with epicentral coordinates 74,391°W and 45,517°S at a depth of 30 km, according to the National Seismological Center ([www.sismologia.cl](http://www.sismologia.cl)). This earthquake is the largest recorded in the country since that occurred on September 16, 2015 (Illapel, Mw=8.4). The geometry of the fault -or focal mechanism- and its location are consistent with the subduction of the Nazca plate under the South American plate. Preliminary estimates, based on scaling relationships - indicate that the rupture length reaches about 60 km with an average fault slip of around 2 m. This earthquake takes place in a region where earthquakes of the same type have prior occurrence, such as the giant earthquake of May 22, 1960, with an estimated magnitude of 9.5 (Kanamori and Cipar, 1974). Maximum accelerations in the order of 27% g have been recorded in the horizontal east-west component of the GO07 station located in the southern part of the island of Chiloé, near Quellón. A GNSS (Global Navigation Satellite System) device placed at the same site, was subjected to a co-seismic displacement of 17 cm to the west, 4 cm to the south and 7 cm of subsidence.

### Tectonic Context

The seismicity of Chile is mainly dominated by the convergence between the Nazca and South American plates, at a rate between 6.5 and 7 cm/yr. South of the Taitao Peninsula (~46°S), it is the Antarctic plate that subducts beneath the South American plate at a rate of approximately 1.8 cm/yr. In the southernmost region, the Magallanes-Fagnano Fault, which coincides with the Strait of Magellan in its western sector and continues eastward along Fagnano Lake, accommodates a left-lateral movement, of the order of 0.7 cm/yr between the Scotia and South American plates. The large relative convergence velocity between the Nazca and South America plates is responsible for not only the high seismic productivity -one of the largest in the world- but also for the great dimensions that earthquakes reach in this region.

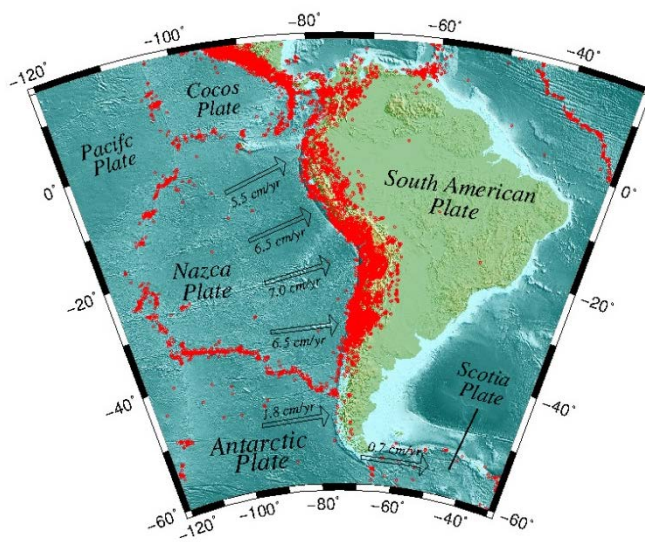


**Fig. 1.** Tectonic context of South America. The Nazca plate converges and subducts beneath the South American plate at about 6.5 to 7 cm each year. Further south, the Antarctic plate does so at 1.8 cm/yr. In austral Chile and Argentina, the Magallanes-Fagnano Fault accomodates about 0.7 cm/yr of left-lateral movement between the Scotia and South American plates.

This relative movement between plates does not take place continuously at their point of interaction. In the case of Chile, this occurs at discrete intervals along the contact surface, which corresponds to an inclined plane between the trench, that geographical feature located about 90-150 km west of the coast, and the point where the Nazca plate reaches a depth of about 50 km. The width of this inclined zone (roughly 19° dip to the east) is of about 150 km. Therefore, large earthquakes ( $M_w$  larger than 7 $\frac{3}{4}$ ) can only grow larger in a north south direction. These large earthquakes with large fault displacements, can generate significant tsunamis due to the potential vertical deformation of the ocean floor.

## Epicentral location and rupture region

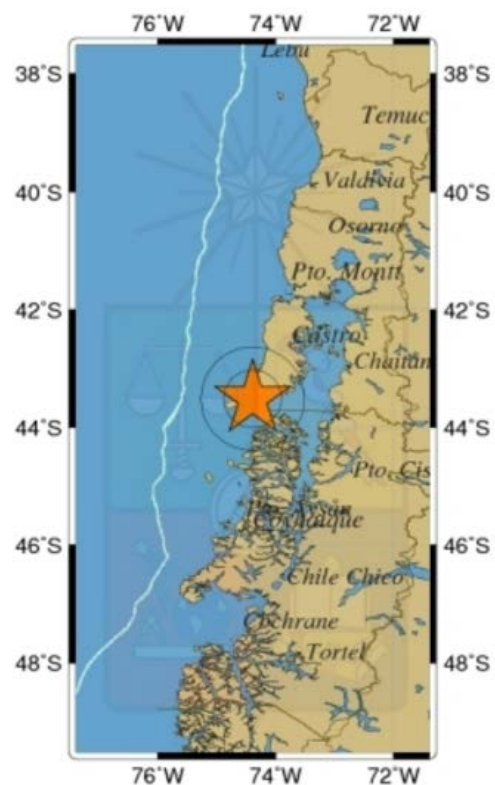
The hypocentral coordinates of the December 25 earthquake are as follows:

Agency	Origin Time	Latitude	Longitude	Depth (km)	Magnitude
CSN	14:22:23	-43.517	-74.391	30.0	7.6 Mw
USGS (NEIC)	14:22:26	-43.416	-73.951	35.1	7.6 Mw
GFZ	14:22:26	-43.38	-73.83	33	7.6 Mw
GCMT Project	14:22:37	-43.54	-734.57	34.2	7.5 Mw, 7.5 Ms

Each agency reports different coordinates, depth and magnitude, since they use different stations, wave propagation velocity models and magnitude estimation methods. The CSN reports  $M_w$  based on the estimated W-phase method with stations near the epicenter, but at distances greater than  $5^\circ$  (about 550 km), in this case the report includes 130 information channels, which are all nearby stations. The USGS (NEIC) uses the same method but also with global stations. GeoForschungsZentrum (GFZ) uses its own estimates based on the inversion of the moment tensor and also by the method discussed above, while the GCMT Project inverts the moment tensor using long and intermediate period waves.

The final hypocentral report, published on the website of the CSN ([www.sismologia.cl](http://www.sismologia.cl) or [www.csn.uchile.cl](http://www.csn.uchile.cl)), shows the map and characteristics of the earthquake as shown in Fig. 2.

**Fig. 2.**  
**Sismo 25 de diciembre de 2016**  
Hora origen: 14:22:23  
Latitud: -43.517  
Longitud: -74.391  
Profundidad: 30 km  
 $M_w = 7.6$   
Referencia geográfica: 67 km al nor-oeste de Melinka.



The hypocentral coordinates indicate a location 67 km north-west of the town of Melinka, Guaitecas Islands, at 30 km depth. This point corresponds to the beginning of the rupture, which extends about 60 km to the north. The zone of rupture can be understood as an area (almost a surface) in the contact between the Nazca and South American plates corresponding, in this case, to the region of approximately 60 km in length located at the south-west end of Chiloe Island. Figure 3 shows the amplitude of expected ground motion given the magnitude and location of the earthquake, using attenuation relationships of acceleration  $v/s$  distance recently developed for Chile (Montalva et al, 2017). As expected, maximum values of ground movement in acceleration and velocity, hence in Instrumental Intensity, occur in the vicinity of the epicentral region.

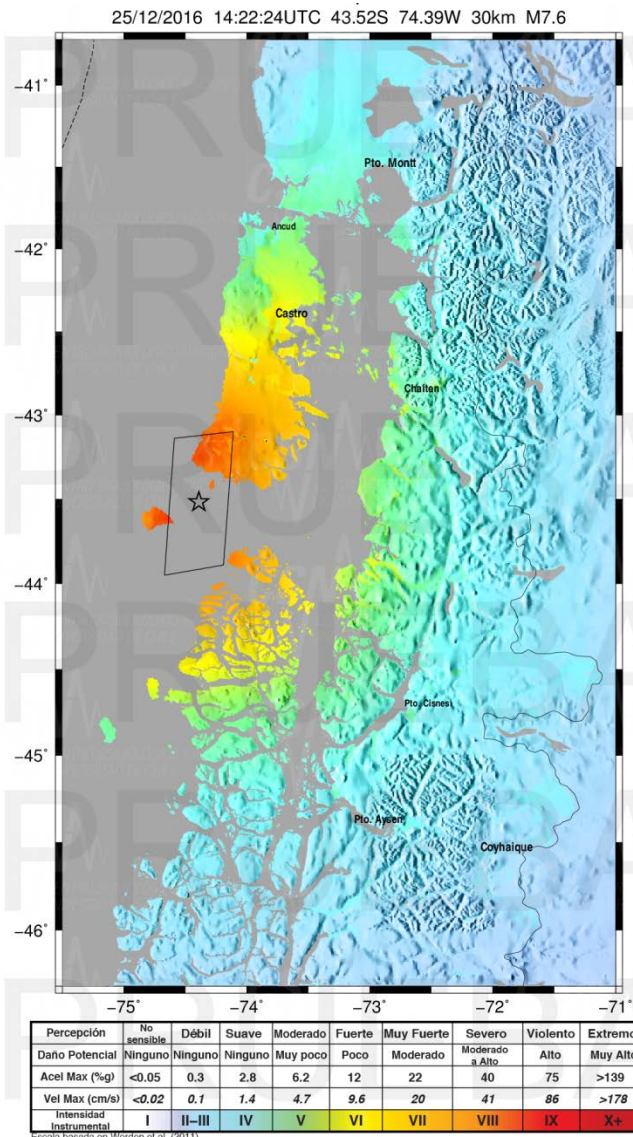


**Fig. 3.** Preliminary estimation of the location of the fault - based on scale-to-magnitude relationships - and the consequent estimation of the ground movement level due to the earthquake of December 25, 2016. The epicenter is shown as the black star. The ground motion is proportional to the color following the scale at the bottom.

## Observed Accelerations and Earthquake Characteristics

The recently established National Network of Accelerometers has been tested for the first time in this region, where large earthquakes occur infrequently. Figure 4 shows the records of the east-west horizontal component generated by the earthquake. The peak ground acceleration recorded at LL07 (Espejo de Luna) station reached 19% of the acceleration of gravity (g) while in the town of Quellón it reached its maximum, 27% g.

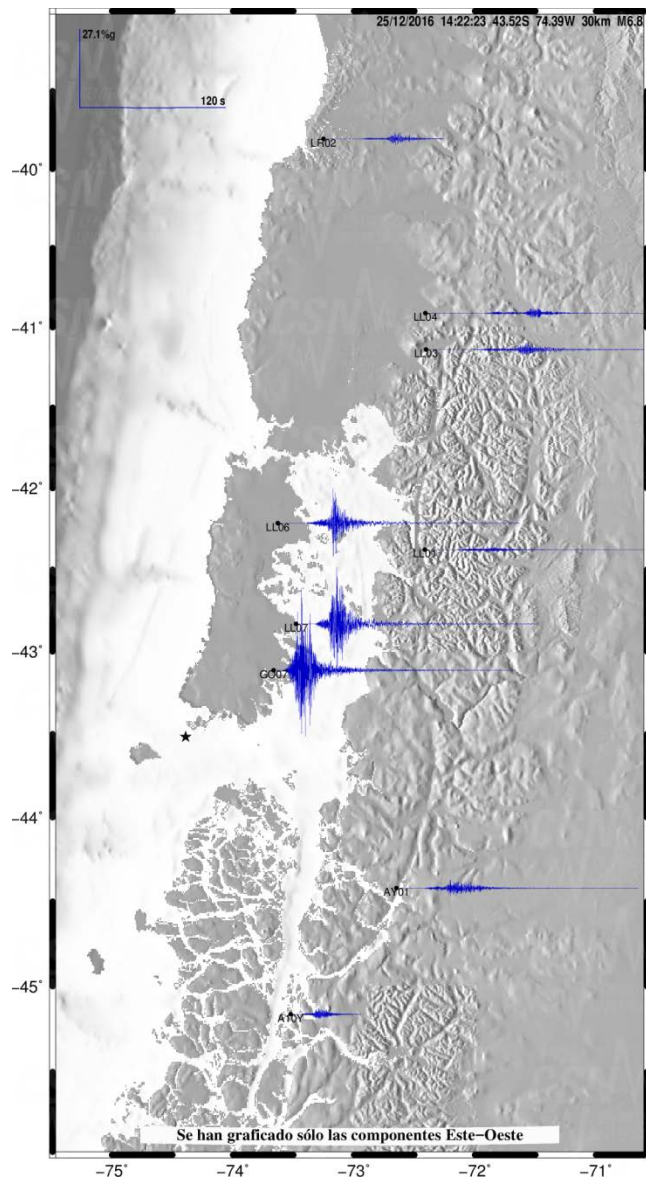
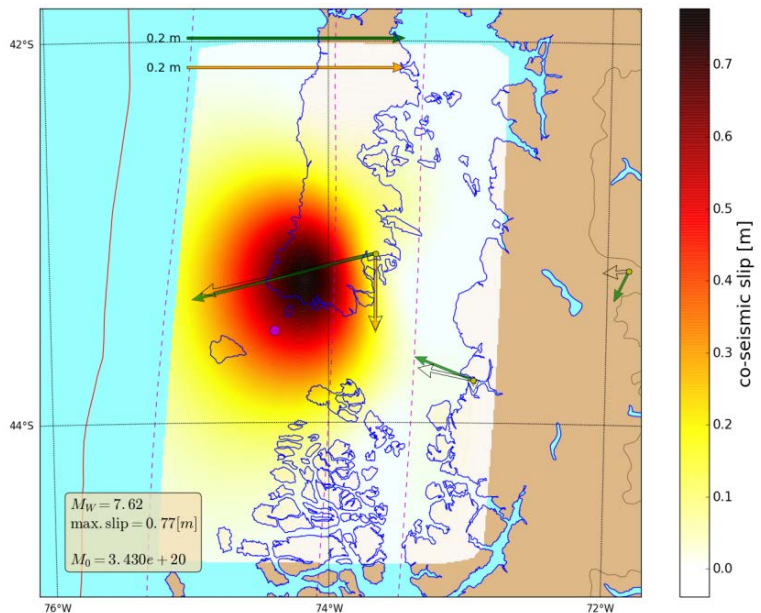


**Fig. 4.** Horizontal acceleration records (east-west component) produced by the earthquake  $M = 7.6$  of December 25, 2016. The black star represents the location of the epicenter of the earthquake. The maximum acceleration reaches 19% of the acceleration of gravity in the station LL07 (Espejo de Luna), in the Island of Chiloé (Figure prepared by F. Leyton).

Digital strong motion records of this, and previous earthquakes, (three components at 100 samples per second) are available on the CSN website at <http://evtdb.csn.uchile.cl/>. This site contains a complete database with all the acceleration data that has been recorded by the CSN and Collaborative Networks (Integrated Plate Boundary Observatory Chile (IPOC) in northern Chile and Geophysical Research Observatories, GRO). It is possible that the acceleration database produced by this earthquake will be expanded, after visits for maintenance and data extraction at those stations still not connected to the CSN network. Continuous records of broadband seismometers of all stations are available at [www.iris.edu](http://www.iris.edu) (networks C, C1 and CX).

On the other hand, the observations of slip in the fault inferred from the Satellite Global Navigation System (GNSS) are shown in Figure 5. Maximum values of displacement in the surface of the Earth are observed in the station located in Quellón, reaching displacements of the order of 17 cm to the west and 4 cm to the south. It is also possible to observe co-seismic displacements of the order of 6 cm towards the northwest in the locality Raúl Marín Balmaceda. These values -and the location of maximum horizontal displacement at the southwestern end of Chiloé Island- will be most likely confirmed by Interferometric Synthetic Aperture Radar (InSAR) images which will be available soon.

**Fig. 5.** The green vectors represent the horizontal static movement (or displacement at the Earth's surface) associated to the earthquake of 25<sup>th</sup> December, 17 cm towards the west in Quellón; the yellow vector at the same place shows a subsidence of the order of 7 cm. The colors, ranging from yellow to intense red represent the estimate of the location of slip in the rupture zone, revealing a seismic moment of  $3.4 \times 10^{20}$  N-m which is equivalent to a magnitude of 7.6; equivalently, larger fault displacement -up to several meters- can be accommodated in a smaller total area maintaining the total moment. (Figure prepared by F. del Campo).



In this calculation, it is assumed that slip on the fault occurs along the contact plane between the two plates given by Hayes et al. (2010). The hypocenter is located at the southern end of maximum slip, a similar scenario is observed for other recent earthquakes in Chile (Illapel, 2015, Iquique, 2014 and Maule, 2010). In all three cases, rupture begins at places away from maximum displacement. Considering a convergence rate of 6.5 cm/year, in the 56 years since the last 1960 earthquake in this area, an equivalent displacement of 3.6 m has been accumulated.

## Earthquake Duration

When plate boundary earthquake occurs in Chile, the sliding of the Nazca plate under the South American plate does not take place simultaneously along the entire rupture surface. The rupture propagates from the hypocenter in a preferred direction - in this case to the north - with speeds of the order of 2 to 3 km/s, therefore it is expected to take between 20 to 30 s to propagate along a rupture of 60 km. As Fig. 5 displays, the rupture is not uniform, but shows a maximum displacement north of the hypocenter. The location of the maximum fault displacement point precisely to the place where the maximum seismic moment release is located. From seismograms recorded at seismic stations located in different azimuths and distances, it is possible to solve how the seismic moment is released as a function of time once the rupture has begun. Fig. 6 shows a comparison of the source time functions for the most recent large earthquakes that have taken place in Chile: December 25, 2016; September 16, 2015; April 1, 2014; and February 27, 2010. For the most recent event, the rate of release of moment is maximum between 0 and 20 s reaching a maximum of  $2.92 \times 10^{19}$  Nm, while that of the 2010 earthquake extends for more than 100 sec reaching a maximum rate of seismic moment release of more than 10 times the former.

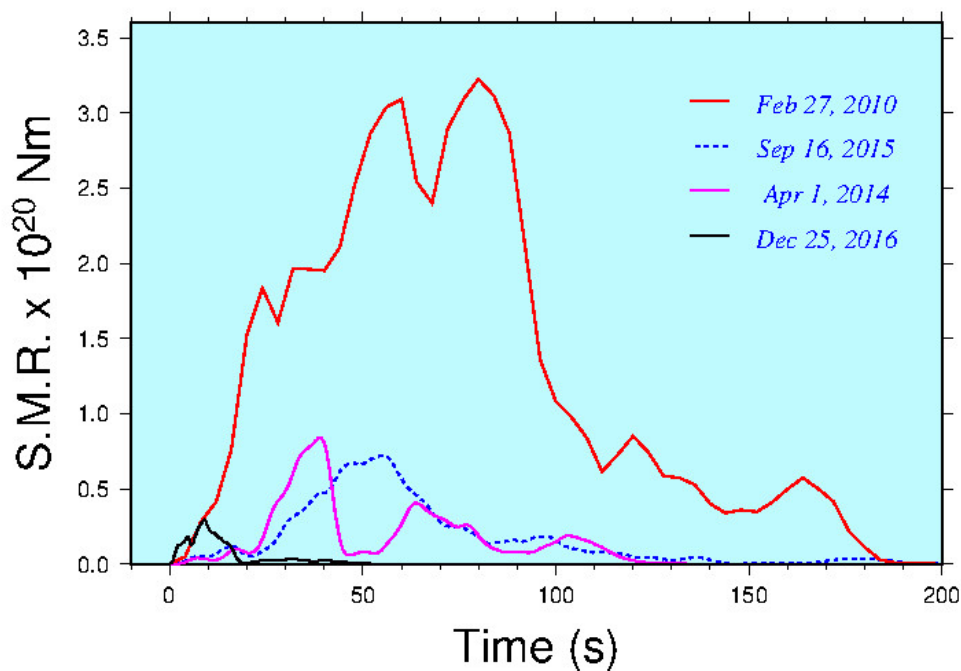


Fig. 6.

Comparison of the seismic moment release rate (SMR) for the last four large subduction earthquakes in Chile:  $M_w = 8.8$  from February 27, 2010,  $M_w = 8.4$  from September 16, 2015,  $M_w = 8.2$  from April 1, 2014 and the  $M_w = 7.6$  of December 25, 2016. The duration of the latter is no more than 20 s and its amplitude is about 10 times lower than that of February 27, 2010. The seismic moment of each event corresponds to the area under each curve. Data provided by G. Hayes (USGS).

## Aftershocks

Most plate boundary earthquakes of significant magnitude generate a number of aftershocks, understood as an earthquake of lesser magnitude that occurs in a volume close to the fault that has been activated in response to the change of stress generated by the mainshock. Although there are several approaches to define the volume, one common approach is to estimate the length of the rupture associated with the mainshock and extend that dimension from both ends of the fault. All the earthquakes contained in this new region, of magnitude smaller than the magnitude of the main earthquake, can be considered as aftershocks. The left panel of the map in Fig. 7 shows the location of the aftershocks in relation to the epicenter of the main earthquake (red star). The panel on the right shows the evolution of the seismicity of the region as a function of time and latitude since 2010. a large number of aftershocks can be observed around the zone of greater displacement. One week after the main event, the largest magnitude aftershock reaches a value of 5.2 and occurs immediately after the main earthquake; Until 9:00 am on January 1 2017, 86 aftershocks were recorded with magnitude 3.0 or higher.

**Table I.** Aftershocks until 9:00 a.m. (local) on January 1, 2017

Magnitude <b>M</b>	N° events with mag >M
3	86
4	23
5	1
6	0

During the first day, more than 20 aftershocks (nine of them with  $M$  greater or equal than 4.0) were recorded, this is an expected value for an earthquake of this magnitude. Given most of other earthquake sequences in Chile, the future scenario is that aftershocks -in the vicinity of the area directly affected by the earthquake- will continue to take place for several weeks, even months, decreasing its frequency of occurrence. Instrumentally, these aftershocks will take place for several months, where some of them will be felt by the population of the surrounding area especially during the first weeks.

The same figure shows the focal mechanism and the fault plane obtained through the modeling of the seismic source as an ellipse (Vallée and Bouchon, 2004; Di Carli et al., 2010). This process considered the accelerograms of the stations: LL07, LL06, LL01, AY01, LL02, LL04, LR02 and LR03 (see location of these stations in Fig. 4 or at [www.csn.uchile.cl](http://www.csn.uchile.cl)). This modeling corresponds to a kinematic inversion of the rupture propagation where the fault plane is considered an ellipse, assuming a Gaussian slip distribution, with maximum slip at the center of the ellipse. In addition, the estimated focal mechanism is shown in the same figure with a magnitude estimate of  $M_w = 7.7$ . This approach took 13 minutes from the occurrence of the event. In the same figure, the focal mechanism obtained by the methodology of the W-Phase inversion is shown. In this case, a stable solution was found seven and a half minutes after origin time, with a moment magnitude of 7.57, five minutes later, 130 channels of information confirmed this estimation.

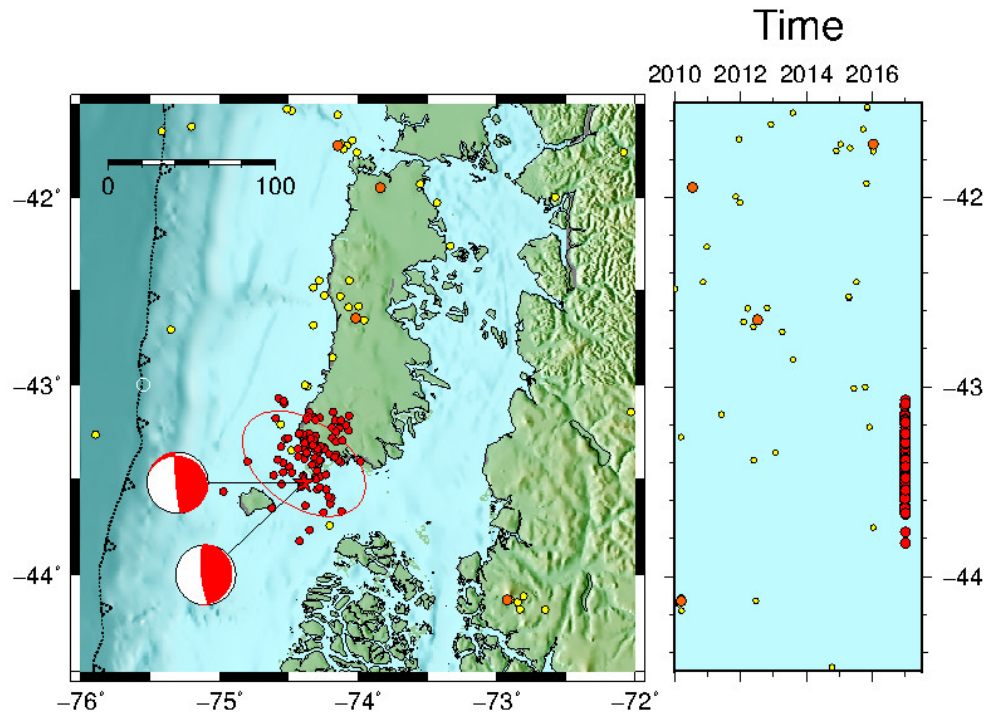


**Fig. 7.** Map and latitude-time views. Seismicity since 2010 in the Chiloé region (yellow circles); earthquakes of magnitude equal or greater than 5 are represented by orange circles. The red circles represent the aftershocks taking place during the first three days. The focal spheres show the type of geometry estimated from two methods: W-Phase (lower sphere, S. Riquelme) and method of ellipses (F. Leyton, upper sphere).

## Discussion

The December 25 2016 earthquake corresponds to an  $M_w=7.6$  interplate event between the Nazca and South American plates. The epicenter is located 67 km north-west of the town of Melinka, at the geographic coordinates  $74.391^\circ\text{W}$ ,  $45.517^\circ\text{S}$ , and 30 km depth.

The previous large event taking place in this region was the May 22, 1960,  $M_w$  9.5 giant earthquake. According to Plafker and Savage (1970) -which documented the changes of elevation of the coast and along inland leveling lines as well as the few observations of horizontal deformations associated to this earthquake- and Cifuentes (1989), the extension of the rupture zone extends from the Arauco Peninsula in the north ( $\sim 37^\circ\text{S}$ ) to the Taitao Peninsula ( $\sim 46^\circ\text{S}$ ) in the south. The average displacement of the earthquake generating fault reached 20 m, with maximum values of more than 40 m (Fig. 8, Barrientos and Ward, 1990). Cisternas et al. (2005), based on data from tsunami deposits at the mouth of the Maullín river, evidence that five events with similar tsunamigenic characteristics have take place in the area within the last 2000 years, with recurrence periods of the order of 300 years. Fig. 8 shows the location of the displacement associated to the earthquake of December 2016 (yellow contour line above the aftershocks, represented by red circles) estimated

from the GNSS displacement observations at the stations located in Quellón, Futaleufú and Raúl Marín Balmaceda respectively. The same displacement curves estimated from the deformations observed for the 1960 earthquake are also presented in blue.

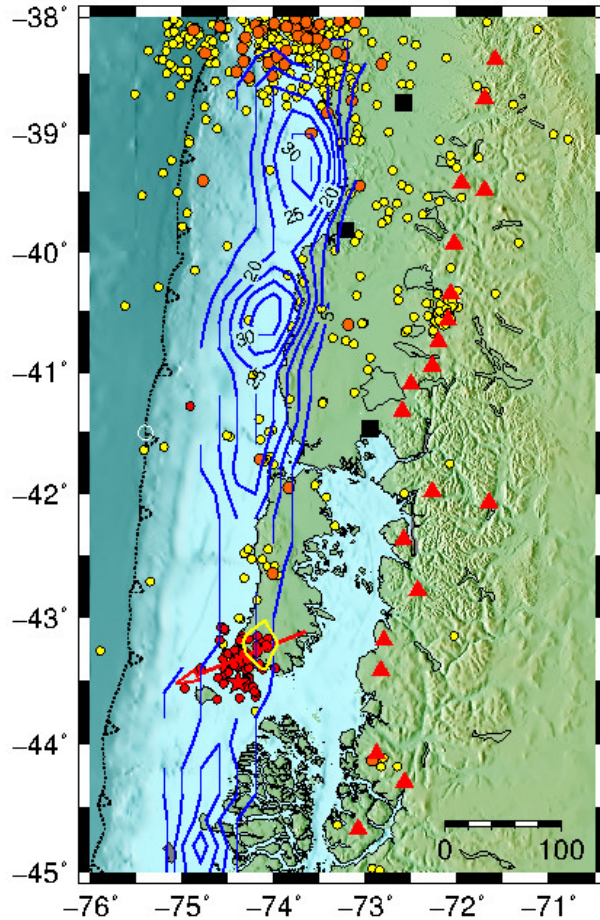


**Fig. 8.** shows the location of the displacement associated with the earthquake of December 2016 in relation to the aftershocks and also the distribution of displacement estimated by Barrientos and Ward (1990) for the earthquake of 1960. It is observed that the earthquake of 2016 locates in an area where there was a slip of the order of 10 m in 1960.

This displacement is considered of relatively smaller size since the maximum displacements (of the order of 40 m) are reached off the coast of Valdivia and a little further south. Given the magnitude of the earthquake of 1960, it is very unlikely that there will be another similarity in this region in the coming decades. It takes hundreds of years to accumulate displacement equivalent to 40 m. However, it is possible that earthquakes of magnitude  $7\frac{1}{2}$  can occur practically anywhere in the country at any time.

## References

- Abe, K.,(1979). Size of great earthquakes of 1837-1974 inferred from tsunami data, *J. Geophys. Res.*, **84**, 1561-1568.
- Abe, K, (1989). Quantification of tsunamigenic earthquakes by the  $M_s$  scale *Tectonophysics*, **166**, 21-34.
- Barrientos S. E. and S.N. Ward, 1990. The 1960 earthquake: Inversion from slip distribution from surface deformation, *Geophys. J. Int.* 103, 589-598.
- Barrientos S. E., G. Plafker and E. Lorca, 1992. Post-seismic coastal uplift in southern Chile *Geophys. Res. Lett.*, 19, 710-704.
- Beck, S., S. Barrientos, E. Kausel, M. Reyes (1998), Source characteristics of historic earthquakes along the central Chile subduction zone, *J. South Am. Earth Sci.*, **11**, 115-129
- Cifuentes, I. L., The 1960 Chilean earthquakes, *J. Geophys. Res.*, **94**, 665 – 680, 1989.
- Cisternas, M.,Torrejón, F., Sawai Y., Machuca G., Lagos M., Eipert A., Youlton C., Salgado I., Kamataki T., Shishikura M., Rajendran C.P., Malik J.K., Rizal Y y M.Husni (2005). Predecessors of the giant 1960 Chile earthquake, *Nature*, **437**, 404-407.
- Di Carli, S., C. François-Holden, S. Peyrat, and R. Madariaga (2010), Dynamic inversion of the 2000 Tottori earthquake based on elliptical subfault approximations, *J. Geophys. Res.*, 115, B12328, doi:10.1029/2009JB006358.
- Kanamori, H. and J.J. Cipar (1974). Focal process of the great Chilean earthquake of May 22, 1960. *Phys. Earth and Planet. Int.* **9**, 128-136.
- Kelleher, J. A. (1972). Rupture zones of large South American earthquakes and some predictions. , *J. Geophys. Res.*, **77**, 2087-2103.
- Montalva, G., Bastías, N. y A. Rodríguez-Marek (2017) Ground Motion Prediction Equation for the Chilean Subduction Zone. *Bull. Seism. Soc. Am.*, *en prensa*.
- Lomnitz, C. (2004) Major earthquakes of Chile: A historical survey, 1535 to 1960, *Seism. Res. Lett.*, **75**, 368-378.
- Plafker, G. and J. C. Savage, 1970. Mechanism of the Chilean earthquakes of May 21 and 22, 1960, *Geol. Soc. Am. Bull.*, 81, 1001-1030
- Vallée, M., and M. Bouchon (2004), Imaging coseismic rupture in far field by slip patches, *Geophys. J. Int.*, 156, 615–630.